The remaining skeletal modes show small downshifts. The mode at 1596 cm^{-1}, localized on the phenyl ring, does not shift, consistent with the expected lack of significant phenyl conjugation, the peripheral phenyl groups being twisted out of the porphyrin plane; steric hindrance with the pyrrole C_bH atoms provide a substantial barrier to rotation.[23] This observation strengthens the inference[24] that the resonance enhancement of the phenyl modes in TPP is due not to ground-state conjugation but rather to a displacement of the phenyl rings toward coplanarity in the excited state.

The substantial back-donation implied by the porphyrin frequency shifts in the bis(pyridine) adducts are consistent with the molecular orbital calculations of Gouterman and co-workers.[2,3] Replacement of pyridine by CO abolishes the back-bonding effects on the porphyrin frequencies; the frequencies displayed by the CO adducts of RuOEP are just those expected on the basis of the porphyrin core size. Thus, CO competes very effectively with porphyrin for the Ru $d\pi$ electrons. Indeed, the bound CO so dominates the electronic structure that the same porphyrin frequencies are seen whether the trans axial ligand is pyridine or MeOH or when there is no trans ligand at all. Direct evidence for the strong back-donation to CO is seen in the C–O stretching frequency, 1930 cm^{-1}, which is 30 cm^{-1} lower than that shown by $Fe^{II}PP(CO)(ImH)$ in the same solvent, CH_2Cl_2.[15] The Ru–CO frequency 513 cm^{-1}, is 18 cm^{-1} higher than the Fe–CO stretch of this complex.[15] For the same force constants, a somewhat lower M–CO frequency would be expected for the Ru adduct, due to the greater metal atom mass. Thus, the frequency upshift actually observed is an indication of significantly stronger bonding, consistent with greater back-donation to CO from Ru^{II} than from Fe^{II}.

The observation of the Ru–C–O bending mode at 578 cm^{-1} is of interest. This band has been observed in several heme proteins,[15,16] but it is not seen in protein-free heme CO complexes except in the case of a strapped porphyrin,[25] and the observation of this band has therefore been associated with tilting of the Fe–C–O linkage.[15] There is no reason to expect the Ru–C–O linkage to be tilted in RuOEP(CO)(py), and in this case the observation of the bending mode in the RR spectrum must be a purely electronic effect, perhaps associated with the increased back-donation from Ru.

Acknowledgment. We thank Professor Dewey Holten for samples of $Ru(OEP)(py)_2$ and $Ru(TPP(py)_2$ and for helpful discussions. Special thanks are extended to Kwang-Hyun Ahn who provided $RuTPP(CO)(CH_3CN)$ and $RuTPP(py)_2$. This work was supported by Grant AC02-81ER10861 from the U.S. Department of Energy.

Registry No. $Ru(TPP)(py)_2$, 34690-41-0; Ru(TPP)(CO)(py), 41751-82-0; Ru(TPP)(CO)(MeOH), 89555-37-3; $Ru(OEP)(py)_2$, 54762-60-6; Ru(OEP)(CO)(py), 38478-17-0; Ru(OEP)(CO)(MeOH), 89530-39-2.

(23) Eaton, S. S.; Eaton, G. R. *J. Am. Chem. Soc.* **1975**, *97*, 3660.
(24) Burke, J. M.; Kincaid, J. R.; Spiro, T. G. *J. Am. Chem. Soc.* **1978**, *100*, 6077–6083.
(25) Yu, N.-T.; Kerr, E. A.; Ward, E. B.; Cheung, C. K. *Biochemistry* **1983**, *22*, 4534.

Contribution from the Dipartimento di Scienze Chimiche, University of Catania, 95125 Catania, Italy, and Dipartimento di Chimica Inorganica, Metallorganica ed Analitica, University of Padova, 35100 Padova, Italy

Electronic Structure of Transition-Metal Tetracoordinated Complexes. 1. Theoretical ab Initio and UV–Photoelectron Spectroscopy Study of Palladium(II) and Platinum(II) Square-Planar Acetylacetonate Complexes

Santo Di Bella,[1a] Ignazio Fragalà,*[1a] and Gaetano Granozzi*[1b]

Received August 8, 1985

The electronic structures of $Pd(acac)_2$ and $Pt(acac)_2$ have been studied by using the pseudopotential valence-only ab initio method (including corrections for the major relativistic effects in the case of the heavier metal complex) and combined He I and He II photoelectron spectroscopy. A remarkable metal–ligand covalency involving orbitals of σ and π symmetry emerges from the analysis of the theoretical results. In particular, interactions with orbitals of σ symmetry involve empty s and d_{xy} metal orbitals and results in important ligand-to-metal charge transfer. These effects are both of a major importance in the case of the Pt complex. Detailed assignments of the UV photoelectron spectra are proposed on the basis of results of a simple perturbative treatment to correct the Koopmans eigenvalues for the reorganization effects in the ion states. Ionization energy values associated to production of selected ion states have been also evaluated by a ΔSCF treatment. The relative intensity changes of low-ionization-energy photoelectron bands observed on passing from the He I to the He II excited spectra have proven to be crucial guidance for the final assignments.

Introduction

Considerable attention has been focused on the electronic structures of tetracoordinated square-planar complexes of d^8 metal(II) ions. Efforts have been directed to rationalize their high reactivities and kinetical labilities[2] as well as to understand their anticancer[3] and unusual solid-state electric properties.[4] Nevertheless, the large number of investigations have left still uncertain the energy sequence of the upper filled molecular orbitals (MO's).[5]

In this context, UV–vis optical spectroscopy was first used within a crystal field methodological approach.[5c,d,6] However, it quickly became evident that this approach was only capable of providing the sequence of electronic excitations rather than of MO energy levels.[7] Later on, gas-phase UV photoelectron spectroscopy (PES) data were used, within the Koopmans' approximation,[8] to map the energy of the outermost occupied MO's

(1) (a) University of Catania. (b) University of Padova.
(2) (a) Hartley, F. R. *The Chemistry of Platinum and Palladium*; Wiley: New York, 1973. (b) Belluco, U. *Organometallic and Coordination Chemistry of Platinum*; Academic: London, 1974. (c) Bishop, K. C., III. *Chem. Rev.* **1976**, *76*, 461.
(3) (a) Prestayko, A. W., Crooke, S. T., Carter, S. K., Eds. *Cisplatin: Current Status and New Developments*; Academic: New York, 1980. (b) Stettenko, A. I.; Presnov, M. A.; Konovalova, A. L. *Russ. Chem. Rev. (Engl. Transl.)* **1981**, *50*, 353.
(4) See for example: (a) *Extended Linear Chain Compounds*; Miller, J. S., Ed.; Plenum: New York, 1982; Vol. 1, 2; 1983; Vol. 3. (b) Glieman, G.; Yersin, H. *Struct. Bonding (Berlin)* **1985**, *62*, 87.
(5) (a) Gray, H. B.; Ballhausen, C. J. *J. Am. Chem. Soc.* **1963**, *85*, 260. (b) Nishida, Y.; Kida, S. *Coord. Chem. Rev.* **1979**, *27*, 275. (c) Vanquickenborne, L. G.; Ceulemans, A. *Inorg. Chem.* **1981**, *20*, 796. (d) Attanassov, M. A.; Nikolov, G. St. *Inorg. Chim. Acta* **1983**, *68*, 15.
(6) Fenske, R. F.; Martin, D. S., Jr.; Ruedenberg, K. *Inorg. Chem.* **1962**, *1*, 441.
(7) Veillard, A.; Demuynck, J. *Modern Theoretical Chemistry*; Schaefer, H. F., Ed.; Plenum: New York, 1977.

0020-1669/86/1325-3997$01.50/0

Table I. PSHONDO Eigenvalues and Population Analysis of Outermost MO's of $Pd(acac)_2$

MO	eigenvalue, eV	% populn[a] Pd 4d	Pd 5s	Pd 5p	O	C	C′	H	H′	overlap populn Pd–O	dominant char
$3b_{2g}$	−8.97	9			41	4	46			−0.034	π_3, d_{xz}
$2b_{1u}$	−9.68			1	34	11	54			0.014	π_3
$8a_g$	−10.74	57	9		29	2	1	2		−0.018	d_{z^2}, n_+
$5b_{2u}$	−11.60				74	8	7	11		0.000	n_-
$2b_{3g}$	−11.76	59			26	15				−0.052	d_{yz}, π_2
$7a_g$	−12.40	54	2		31	5	8			−0.052	$d_{x^2-y^2}$, d_{z^2}, n_+
$6b_{3u}$	−12.87			2	77	5	7	6	3	0.020	n_+
$5b_{1g}$	−12.90	8			64	11	8	8	1	0.014	n_-, d_{xy}
$2b_{2g}$	−12.95	63			19	3	15			−0.016	d_{xz}, π_1
$1a_u$	−14.05				77	23				0.000	π_2
$5b_{3u}$	−14.90			1	39	20	17	8	15	0.010	σ
$1b_{1u}$	−15.62			1	55	32	12			0.008	π_1
$1b_{3g}$	−15.63	40			51	9				0.050	π_2, d_{yz}
$6a_g$	−16.07	53			13	5	17	2	10	0.044	$d_{x^2-y^2}$, n_+
$5a_g$	−16.25	15	1		25	16	15	14	14	0.024	σ, d_{z^2}
$1b_{2g}$	−16.34	27			46	20	7			0.036	π_1, d_{xz}

[a] See Figure 1.

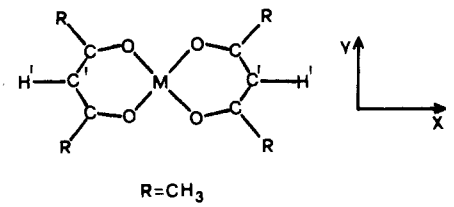

R=CH_3

Figure 1. Geometry adopted for the $M(acac)_2$ complexes.

of square-planar complexes.[9,10] However, the results reported up to now remain controversial because reorganization energies upon ionization have not been taken into account. It is well-known that such effects may be sufficiently large to upset the energy sequence of ground-state MO's.[7,11] Moreover, the more reliable quantum-mechanical calculations (semiempirical,[12] ab initio,[13] and Xα[14]), which are today available for square-planar complexes, all point to strong covalent character in the metal–ligand bonding, which is critically dependent upon prerequisites of both the metal and the ligands. Therefore, there is some reasonable doubt as to whether the metal–ligand bonding of such complexes can be described by a unique general model.

These observations suggest that the best methodological approach to this intriguing matter might be to combine the characteristics of a unique spectroscopy technique that is capable of singling out individual MO's, such as PE spectroscopy, with the results of high-quality MO calculations (Xα or ab initio), which allow an estimate of reorganization energies in the ion states.

These efforts can certainly promote a better understanding of the properties of square-planar complexes especially in the case of complexes of 4d and 5d metal ions whose properties, relative to those of 3d analogues, are still not fully rationalized.

As a part of a current extensive project involving the joint use of ab initio calculations (including estimates of reorganization energies) and of PE data, we report in this paper the results of a study of the electronic structure of complexes of pentane-2,4-dione (hereafter acac)[15] with Pd(II) and Pt(II) ions (Figure 1).

The PE spectra of these complexes have already been studied in our laboratory.[10] Their choice for the present study was, however, suggested by the very good resolution of their PE spectra, especially in the low-ionization-energy (IE) region, which renders feasible a one-to-one comparison with results of the ab initio calculation.

In order to reduce the dimensions of the secular determinant, especially for future applications to very large planar complexes, the valence-only pseudopotential[16] ab initio method has been used.

Experimental Section

The PE spectra were recorded on a PS18 Perkin-Elmer spectrometer modified by the inclusion of a hollow cathode discharge source giving high output of He II photons (Helectros Development Corp.). The spectra were accumulated in the "multiple scan mode" with the aid of a MOSTEK computer directly interfaced to the spectrometer. The energy scale of consecutive scans was locked to the reference values of the Ar and He $1s^{-1}$ self-ionization lines. The spectra were deconvoluted by fitting the spectral profiles with a series of asymmetrical Gaussian curves after subtraction of the background. The area of bands thus evaluated can be affected by errors smaller than 5%.

Computational Details

Ab initio LCAO–MO–SCF calculations were made by using pseudopotentials to simulate all core electrons of each atom. The Durand and Barthelat formalism[17] was chosen. For any atom C, the pseudopotential is expressed through the local operator for each l value

$$W_{l,c}(r) = \sum_i a_i r^{n(i)} \exp(-\alpha r^2)$$

(8) Koopmans, T. *Physica* **1933**, *1*, 104.
(9) (a) Condorelli, G.; Fragalà, I.; Centineo, G.; Tondello, E. *Inorg. Chim. Acta* **1973**, *7*, 725. (b) Cauletti, C.; Furlani, C. *J. Electron Spectrosc. Relat. Phenom.* **1975**, *6*, 465. (c) Brittain, H. G.; Disch, R. L. *J. Electron Spectrosc. Relat. Phenom.* **1976**, *7*, 475. (d) Maier, J. P.; Sweigart, D. A. *Inorg. Chem.* **1976**, *15*, 1989. (e) Cauletti, C.; Furlani, C. *J. Chem. Soc., Dalton Trans.* **1977**, 1068. (f) Andreocci, M. V.; Dragoni, P.; Flamini, A.; Furlani, C. *Inorg. Chem.* **1978**, *17*, 291. (g) Cauletti, C.; Furlani, C.; Storto, G. *J. Electron Spectrosc. Relat. Phenom.* **1980**, *18*, 329. (h) Kitagawa, S.; Moroshima, I.; Yoshikawa, K. *Polyhedron* **1983**, *2*, 43. (i) Granozzi, G.; Zagrande, G.; Bonivento, M.; Michelon, G. *Inorg. Chim. Acta* **1983**, *77*, L229. (j) Granozzi, G.; Vittadini, A.; Sindellari, L.; Ajò, D. *Inorg. Chem.* **1984**, *23*, 702.
(10) Fragalà, I.; Constanzo, L. L.; Ciliberto, E.; Condorelli, G.; D'Arrigo, C. *Inorg. Chim. Acta* **1980**, *40*, 15.
(11) For a discussion of the Koopmans failures in metal complexes see: Böhm, M. C. *J. Chem. Phys.* **1983**, *78*, 7044.
(12) (a) De Alti, G.; Galasso, V.; Bigotto, A. *Inorg. Chim. Acta* **1970**, *4*, 267. (b) Ciullo, G.; Sgamellotti, A. *Z. Phys. Chem. (Munich)* **1976**, *100*, 67. (c) Böhm, M. C. *Z. Phys. Chem. (Munich)* **1982**, *129*, 149. (d) Herman, Z. S.; Kirchner, R. F.; Loew, G. H.; Mueller-Westerhoff, U. T.; Nazzal, A.; Zerner, M. C. *Inorg. Chem.* **1982**, *21*, 46.
(13) (a) Demuynck, J.; Veillard, A.; Vinot, G. *Chem. Phys. Lett.* **1971**, *10*, 522. (b) Demuynck, J.; Veillard, A. *Theor. Chim. Acta* **1973**, *28*, 241. (c) Sano, M.; Kashiwagi, H.; Yamatera, H. *Bull. Chem. Soc. Jpn.* **1982**, *55*, 750. (d) Fischer-Hjalmars, I.; Henriksson-Enflo, A. *Adv. Quantum Chem.* **1982**, *16*, 1. (e) Noell, J. O.; Hay, P. J. *Inorg. Chem.* **1982**, *21*, 14.
(14) (a) Messmer, R. P.; Interrante, L. V.; Johnson, K. H. *J. Am. Chem. Soc.* **1974**, *96*, 3846. (b) Interrante, L. V.; Messemer, R. P. *Chem. Phys. Lett.* **1974**, *26*, 225. (c) Weber, J.; Daul, C.; Von Zelewsky, A.; Goursot, A.; Penigault, E. *Chem. Phys. Lett.* **1982**, *88*, 78. (d) Louwen, J. N.; Hengelmolen, R.; Grove, D. M.; Oskam, A.; DeKock, R. L. *Organometallics* **1984**, *3*, 908.
(15) For a comprehensive report on the chemical and physical properties of metal β-diketonates see: Mehrotra, R. C.; Bohra, R.; Gaur, D. P. *Metal β-Diketonates and Allied Derivatives*; Academic: London, 1978.
(16) For a concise presentation of the pseudopotential method see: Topiol, S.; Moskowitz, J. W.; Melius, C. F. *J. Chem. Phys.* **1978**, *68*, 2364.
(17) Barthelat, J. C.; Durand, Ph.; Serafini, A. *Mol. Phys.* **1977**, *33*, 159. Pélissier, M.; Durand, Ph. *Theor. Chim. Acta* **1980**, *55*, 43.

Table II. Atomic Charges and Orbital and Overlap Populations of $Pd(acac)_2$ and $Pt(acac)_2$ (Values of the Free Anion Ligand in Parentheses)

		acac				
orbital populn	Pd	O	C	C′	H	H′
s	0.338	1.858 (1.888)	1.174 (1.181)	1.089 (1.052)	0.862 (0.992)	0.872 (0.979)
p_σ	0.211	3.081 (3.172)	1.843 (1.829)	1.897 (1.844)		
p_π	0.050	1.657 (1.512)	0.672 (0.775)	1.333 (1.427)		
$4d_\sigma\{x^2-y^2$	1.998					
z^2	1.917					
xy	0.544					
$4d_\pi\{xz$	1.999					
yz	1.970					
charges	+0.973	−0.596 (−0.572)	+0.311 (+0.215)	−0.319 (−0.323)	+0.138 (+0.008)	+0.128 (+0.021)

	Pd–O		C–O		C–C′	
overlap populn	σ	π	σ	π	σ	π
	0.296	0.006	0.516 (0.710)	0.244 (0.336)	0.382 (0.148)	0.242 (0.152)

		acac				
orbital populn	Pt	O	C	C′	H	H′
s	0.612	1.855 (1.888)	1.140 (1.181)	1.129 (1.052)	0.860 (0.992)	0.867 (0.979)
p_σ	0.075	3.089 (3.172)	1.812 (1.829)	1.925 (1.844)		
p_π	0.028	1.670 (1.512)	0.663 (0.775)	1.342 (1.427)		
$5d_\sigma\{x^2-y^2$	2.009					
z^2	1.867					
xy	0.572					
$5d_\pi\{xz$	2.007					
yz	1.948					
charges	+0.882	−0.614 (−0.572)	+0.385 (+0.215)	−0.396 (−0.323)	+0.140 (+0.008)	+0.133 (+0.021)

	Pt–O		C–O		C–C′	
overlap populn	σ	π	σ	π	σ	π
	0.302	−0.030	0.304 (0.710)	0.236 (0.336)	0.580 (0.148)	0.244 (0.152)

Literature values of a_i, $n(i)$, and α parameters have been used.[18] In the case of the Pt atom the pseudopotential[19] includes the major (mass and Darwin) relativistic corrections.[20] Gaussian basis sets (available as supplementary material) have been optimized for each valence shell by a pseudopotential version of the ATOM program.[21] The standard Huzinaga[22] basis sets have been used for hydrogen atoms. The basis sets have been contracted to double-ζ forms (3 + 2 for *n*d and 3 + 1 components for *n*s and *n*p atomic orbitals). Calculations have been carried out by running the PSHONDO program[23] (a modified version of the HONDO program,[24] including pseudopotential) on a Vax-11/780 computer. The geometrical parameters used in the calculations of the anion ligand have been averaged among those of various $(acac)^-$ complexes. Those of $Pd(acac)_2$ and of $Pt(acac)_2$ have been taken from X-ray crystal data[25] optimized to a D_{2h} symmetry. The calculations have been made for model compounds where the methyl groups have been replaced by hydrogen atoms (Figure 1). Present theoretical results always refer to such model complexes. Gross atomic charges and bond overlap populations have been obtained by Mulliken's population analysis.[26] IE's have been corrected for repolarization and correlation term upon ionization using a first-order perturbative treatment (PT).[27] This procedure, although less rigorous than ΔSCF calculations (which, however, neglect the correlation term), requires less computational efforts because only one SCF iteration is required to compute each IE value. Furthermore, selected PT IE's have been compared to values obtained by evaluating repolarization energies associated to production of corresponding ion states through more rigorous ΔSCF calculations, in which the Nesbet operator[28] has been used to solve the open-shell problem. ΔSCF IE's are always comparable to those obtained from the PT (Tables III, V) using a 0.75 factor to scale the PT repolarization energies.

Results and Discussion

Eigenvalues and percentage population analysis of the 16 outermost occupied MO's of $Pd(acac)_2$ are reported in Table I. The atomic charges and relevant orbital and overlap populations are compiled in Table II. To discuss these data, it is worth remembering the qualitative description of relevant valence orbitals of the anion ligand that are mainly responsible for the bonding with the central Pd atom. These are the symmetry combinations of two in-plane lone pairs (n_+ and n_-) of the carbonyl oxygens (a_1 and b_1 in C_{2v}, respectively) and the two more external π MO's ($\pi_3(b_2)$, $\pi_2(a_2)$) extending over the entire acac ligand.[10,29] It is important to include within the π set also a totally symmetric orbital of a_1 symmetry (π_1) that lies more internal.

The energy ordering of above MO's provided by the present calculation is $\pi_3 > n_- > n_+ > \pi_2 > \pi_1$. In the D_{2h} symmetry of the $(acac)_2^{2-}$ cluster each of these MO's give rise to two symmetry combinations of u and g symmetry (Figure 2). Their relative energies depend upon nonbonded interligand repulsions. Of course, only those orbitals having a g symmetry are suitable to interact with the metal 4d subshells.

Population data (Table I) provide information on the metal–ligand bonding and, furthermore, can be used to picture an orbital diagram (Figure 2) for the formation of the complex. In this diagram the energy sequences of uppermost filled valence MO's of $Pd(acac)_2$ and of the $(acac)_2^{2-}$ cluster have been matched[30] in order to reproduce the Pd–O overlap population data of various MO's. It is worth noting that the metal 4d orbitals are strongly admixed with several ligand-based orbitals. Actually, among the 16 upper filled MO's, the Pd 4d subshells provide sizable contributions to 10 MO's (Table I). Of course, among these MO's, each pair of symmetry-related MO's represents, in many cases,

(18) (a) Daudey, J. P.; Jeung, G.; Ruiz, M. E.; Novaro, O. *Mol. Phys.* **1982**, *46*, 67. (b) Blake Ortega, I.; Barthelat, J. C.; Costes-Puech, E.; Oliveros, E.; Daudey, J. P. *J. Chem. Phys.* **1982**, *76*, 4130.
(19) Daudey, J. P., private communication.
(20) Barthelat, J. C.; Pélissier, M.; Durand, Ph. *Phys. Rev. A* **1980**, *21*, 1773.
(21) Roos, B.; Salez, C.; Veillard, A.; Clementi, E. Technical Report No. RJ518; IBM Research: 1968.
(22) Huzinaga, S. *J. Chem. Phys.* **1965**, *42*, 1293.
(23) Daudey, J. P., private communication.
(24) Dupuis, M.; Rys, J.; King, H. F. *J. Chem. Phys.* **1976**, *65*, 111.
(25) (a) Knyazeva, A. N.; Shugam, E. A.; Shkol'nikova, L. M. *J. Struct. Chem.* **1971**, *11*, 875. (b) Katoh, M.; Miki, K.; Kai, Y.; Tanaka, N.; Kasai, N. *Bull. Chem. Soc. Jpn.* **1981**, *54*, 611.
(26) Mulliken, R. S. *J. Chem. Phys.* **1955**, *23*, 1833.
(27) (a) Trinquier, G. *J. Am. Chem. Soc.* **1982**, *104*, 6969. (b) Gonbeau, D.; Pfister-Guillouzo, G. *J. Electron Spectrosc. Relat. Phenom.* **1984**, *33*, 279. (c) Zangrande, G.; Granozzi, G.; Casarin, M.; Daudey, J. P.; Minniti, D. *Inorg. Chem.* **1986**, *25*, 2872.
(28) Nesbet, R. K. *Proc. R. Soc. London A* **1955**, *230*, 312.
(29) Evans, S.; Hammett, A.; Orchard, A. F.; Lloyd, D. R. *Faraday Discuss. Chem. Soc.* **1972**, *54*, 227.
(30) Because of the unbalanced 2− charge, all the eigenvalues of the $(acac)_2^{2-}$ cluster lie, of course, very high in energy.

Table III. Relevant PE Data, Computed IE's, and Assignments of the PE Spectrum of $Pd(acac)_2$

band label	IE, eV exptl	IE, eV ΔSCF[a]	IE, eV PT[a]	rel intens[b] He I	rel intens[b] He II	assignt[c]
A	7.79	8.51 (0.46)	8.71 (0.41)	1.04	1.12	$3b_{2g}$
B	8.38	9.25 (0.43) [d]	9.48 (0.37) [d]	0.65	0.74	$2b_{1u}$
C	8.59	8.80 (1.94) [d]	8.90 (1.94) [d]	1.07	1.86	$8a_g$
D	8.99	10.07 (1.69)	10.20 (1.65)	0.70	1.56	$2b_{3g}$
E	9.25	10.78 (0.82)	10.83 (0.84) [d]	0.95	0.94	$5b_{2u}$
F	9.40		10.73 (1.72) [d]	0.87	1.24	$7a_g$
G	9.65		11.40 (1.62)	1.09	1.38	$2b_{2g}$
H	10.12		12.03 (0.90)	1.00	1.00	$6b_{3u}$
I	10.65		12.24 (0.73)	0.94	0.77	$5b_{1g}$
J	11.30		13.39 (0.77)	0.77	0.63	$1a_u$

[a] The repolarization energy values are reported in parentheses. PT values represent the repolarization contributions (scaled by a 0.75 factor; see text) to the total reorganization energy. [b] The intensity of band H has been taken as reference. [c] See Table I for the dominant character of each MO. [d] The inversion of the theoretical IE sequence is due to experimental He I vs. He II relative intensity data (see text).

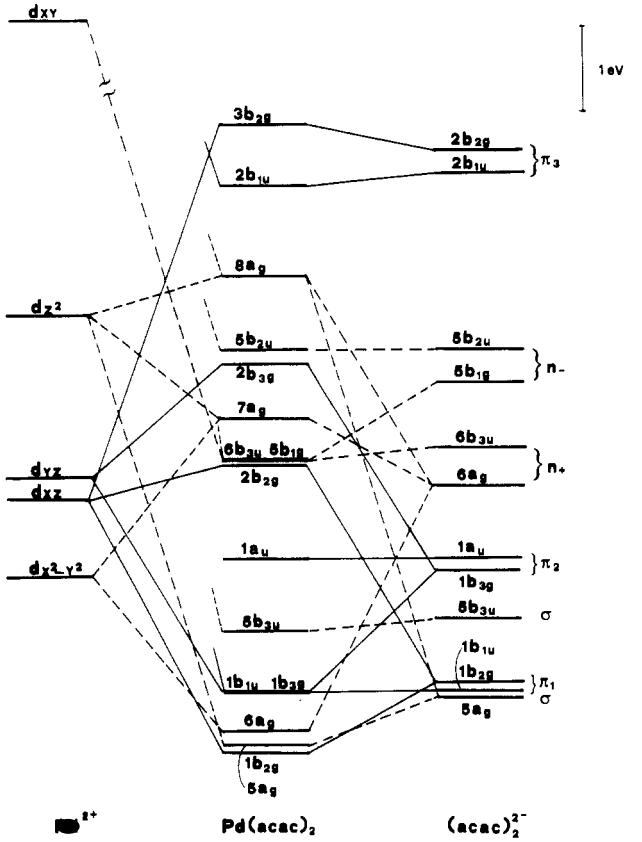

Figure 2. Molecular orbital scheme of $Pd(acac)_2$. σ and π interactions are shown by dashed and solid lines, respectively. Only filled levels are represented.

bonding and antibonding partners within the framework of ligand–Pd interactions (Figure 2).

Of particular interest are the metal–ligand interactions among the orbitals of a_g symmetry that give rise to the three MO's $8a_g$, $7a_g$, and $6a_g$. In the free-ligand anion the more external $6a_g$ orbital lies, in fact, intermediate in energy between the d_{z^2} and $d_{x^2-y^2}$ metal orbitals. Therefore, it might be expected that the resulting $7a_g$ MO (Figure 2) in $Pd(acac)_2$ would posses a total Pd–ligand nonbonding character. By contrast, it is strongly Pd–O antibonding (Table I) because of a stronger interaction with the $d_{x^2-y^2}$ than with the d_{z^2} metal orbital. Moreover, it is noted that the $8a_g$ and $7a_g$ MO's are also admixed with metal 5s orbitals.

The more internal $1b_{2g}$ and $5a_g$ MO's possess a strongly bonding character because of significant interactions with suitable metal subshells. Such bonding interactions have not been recognized in earlier studies.[10,29]

The effects due to the complexation on the electron distributions of the acac ligand and of the Pd atom are summarized in Table II.

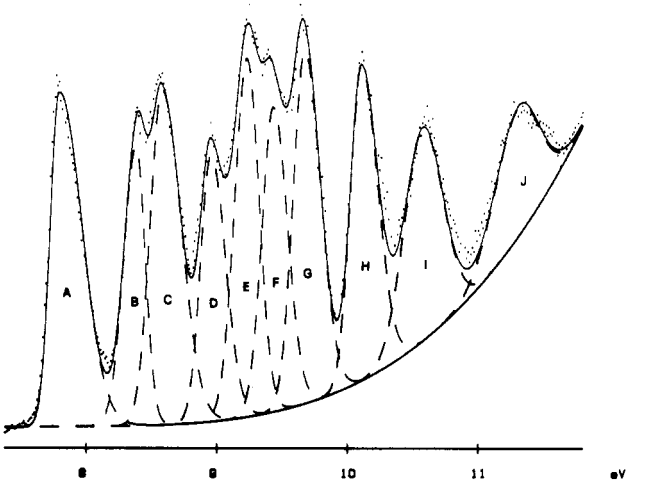

Figure 3. He I spectrum of $Pd(acac)_2$ in the low-IE region: experimental spectrum (point lines), Gaussian components (dashed lines), convolution of Gaussian components (solid line).

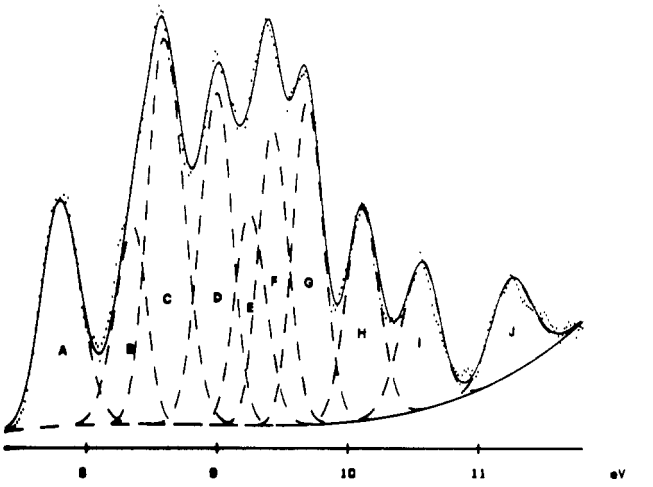

Figure 4. He II spectrum of $Pd(acac)_2$ in the low-IE region: experimental spectrum (point lines), Gaussian components (dashed lines), convolution of Gaussian components (solid line).

The atomic charge of the central Pd atom is indicative of an oxidation state near +1 mainly because of a ligand-to-metal σ donation in the $4d_{xy}$ and 5s metal orbitals. Accordingly, the p_σ population of the ligand carbonyl oxygens decreases with respect to that of the uncomplexed ligand. The effect of the bonded Pd atom on the ligand π population is much more intriguing. Inspection of Tables I and II indicates that, even though many MO's of π symmetry provide some Pd–O overlap population, the resulting total Pd–O π population is vanishing. Such an effect depends upon the filling of all the uppermost bonding and antibonding MO's of π symmetry so that their contributions to the

Table IV. PSHONDO Eigenvalues and Population Analysis of Outermost MO's of $Pt(acac)_2$

MO	eigenvalue, eV	% populn[a] Pt 5d	Pt 6s	Pt 6p	O	C	C′	H	H′	overlap populn Pt–O	dominant char
$3b_{2g}$	−8.96	18			36	4	42			−0.054	π_3, d_{xz}
$2b_{1u}$	−9.79				30	13	57			0.000	π_3
$8a_g$	−9.91	75	15		8	1		1		−0.004	d_{z^2}
$2b_{3g}$	−10.55	75			12	13				−0.064	d_{yz}, π_2
$7a_g$	−11.57	65	1		26	3	3		2	−0.082	$d_{x^2-y^2}$, n_+
$2b_{2g}$	−11.73	65			4	16	15			−0.004	d_{xz}, π_1
$5b_{2u}$	−12.12			1	68	11	9	11		0.004	n_-
$6b_{3u}$	−13.21				78	4	8	6	4	0.000	n_+
$5b_{1g}$	−13.30	7			54	16	12	11		0.022	n_-, d_{xy}
$1a_u$	−14.61				78	22				0.000	π_2
$6a_g$	−15.31	35	1		32	7	13	5	7	0.070	$d_{x^2-y^2}$, n_+
$5b_{3u}$	−15.46				39	19	18	8	16	0.000	σ
$1b_{3g}$	−15.77	23			64	13				0.050	π_2, d_{yz}
$1b_{1u}$	−15.87			1	60	29	10			0.006	π_1
$1b_{2g}$	−16.31	17			53	23	7			0.036	π_1, d_{xz}
$5a_g$	−16.69	7	2		19	15	25	12	20	0.016	σ, d_{z^2}

[a] See Figure 1.

total Pd–O π population almost cancel each other.

The low IE regions (up to 12 eV) of He I and He II PE spectra of $Pd(acac)_2$ are reported in Figures 3 and 4, respectively. They consist of 10 bands (A–J in the figures) whose IE values and relative band areas are reported in Table III.

Remarkable variations of relative band intensities are observed on passing to the He II spectrum. In particular, bands C, D, F, and G become more intense (Table III). Within the Gelius model of PE cross sections,[31] these effects are indicative of sizable contributions of metal 4d AO's in the MO's related to the mentioned bands because literature data on the PE spectra of various acac complexes have unambiguously shown that, first, He I vs. He II relative cross sections of MO's mainly based on the ligand framework are similar and, secondly, that metal d cross sections are greater than those of mentioned MO's under He II radiation.[9g,32]

In Figure 5 experimental and PSHONDO IE's (Koopmans' and PT values) are compared.

As expected, a satisfactory agreement is found between experimental IE's and the theoretical eigenvalues corrected for reorganization effects in the ion state[33] (both ΔSCF and PT) (Table III).

Therefore, we propose the assignment reported in Table III. Band A is assigned to the $3b_{2g}(\pi_3)$ HOMO. The metal 4d contribution to this MO is very small (Table I), and consequently, the relative intensity of the corresponding PE band is unchanged on passing to the He II spectrum. According to calculations (Table III), the next two bands, B and C, should be assigned to the $8a_g$ and $2b_{1u}(\pi_3)$ MO's, respectively. In reality, two experimental observations suggest the opposite ordering $2b_{1u} > 8a_g$. First, band C increases remarkably in relative intensity on passing to the He II spectrum (Table III), thus suggesting a high metal 4d contribution (as is the case of the $8a_g$MO) to the corresponding MO and, secondly, the IE value associated with band B lies near (Table III) that quoted for the unsplit π_3 ionizations in $Zn(acac)_2$[34] (8.34 eV in ref 9h), thus suggesting a analogous assignment.

There is no doubt for the assignment of band D to ionization from the $2b_{3g}$ MO (Table I) because of the remarkable increase in the He II spectrum (Table III). The assignments of bands E and F, however, pose some problems. The calculations would suggest the assignment to $7a_g$ and $5b_{2u}(n_-)$, respectively. Experimental evidence, however, suggests a reversed assignment because (i) the IE's associated to band E lie very close to the value quoted for the unsplit n_- ionizations in $Zn(acac)_2$ (9.29 in ref 9h) and (ii) band F becomes very prominent in the He II spectrum (Table III) in accordance with the high metal 4d character of the $7a_g$ MO (Table I).

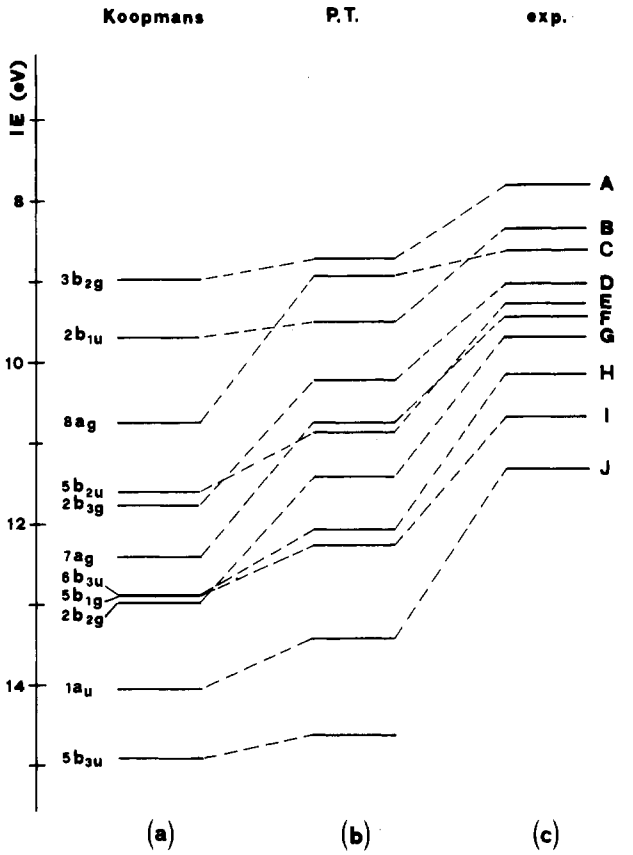

Figure 5. Comparison of Koopmans (a), PT (b), and experimental (c) IE's of $Pd(acac)_2$.

Finally, we assign the next four bands, G–J, to ionization of the $2b_{2g}$, $6b_{3u}(n_+)$, $5b_{1g}(n_-)$, and $1a_u(\pi_2)$ MO's, respectively. Their intensity changes on passing to the He II excitation (Table III) are well tuned to the composition of the corresponding MO's (Table I).

Turning to $Pt(acac)_2$, we note close analogies of theoretical PSHONDO results with those of $Pd(acac)_2$. Of course, small differences in population analyses (Table IV) of various MO's as well as some changes in the energy sequence of uppermost filled

(31) Gelius, U. In *Electron Spectroscopy*; Shirley, D. A., Ed.; North-Holland: Amsterdam, 1972; p 1.
(32) Van Dam, H.; Oskam, A. *J. Electron Spectrosc. Relat. Phenom.* **1979**, *17*, 353.
(33) Due to omission of the terminal methyl groups in the model adopted for calculation, we expect a shift toward higher IE of the computed IE's, especially in the case of the $1a_u$, $2b_{1u}$, and $3b_{2g}$ π MO's.
(34) The $Zn(acac)_2$ complex shows a pseudotetrahedral arrangement, and the chromophore π_3 and n_- levels are degenerate by symmetry (see ref 10).

Table V. Relevant PE Data, Computed IE's, and Assignments of the PE Spectrum of $Pt(acac)_2$

band label	IE, eV			rel intens[b]		
	exptl	ΔSCF[a]	PT[a]	He I	He II	assignt[c]
A	7.60	8.46 (0.50) [d]	8.61 (0.47) [d]	1.17	1.16	$3b_{2g}$
B	8.28	7.78 (2.13) [d]	7.75 (2.25) [d]	0.60	0.95	$8a_g$
C	8.54	8.58 (1.97)	8.66 (1.99)	1.18	1.46	$2b_{3g}$
D	8.90	9.36 (0.43)	9.59 (0.37)	0.90	0.92	$2b_{1u}$
E	9.27		9.60 (2.06)	0.86	1.53	$7a_g$
F	9.70	10.31 (1.42)	10.34 (1.46)	1.07	1.22	$2b_{2g}$
G	9.85		11.53 (0.66)	0.89	0.75	$5b_{2u}$
H	10.43		12.44 (0.83)	1.00	1.00	$6b_{3u}$
I	10.90		12.83 (0.53)	1.04	0.93	$5b_{1g}$
J	11.71		13.93 (0.79)	0.79	0.58	$1a_u$

[a] The repolarization energy values are reported in parentheses. PT values represent the repolarization contributions (scaled by a 0.75 factor; see text) to the total reorganization energy. [b] The intensity of band H has been taken as reference. [c] See Table IV for the dominant character of each MO. [d] The inversion of the theoretical IE sequence is due to experimental He I vs. He II relative intensity data (see text).

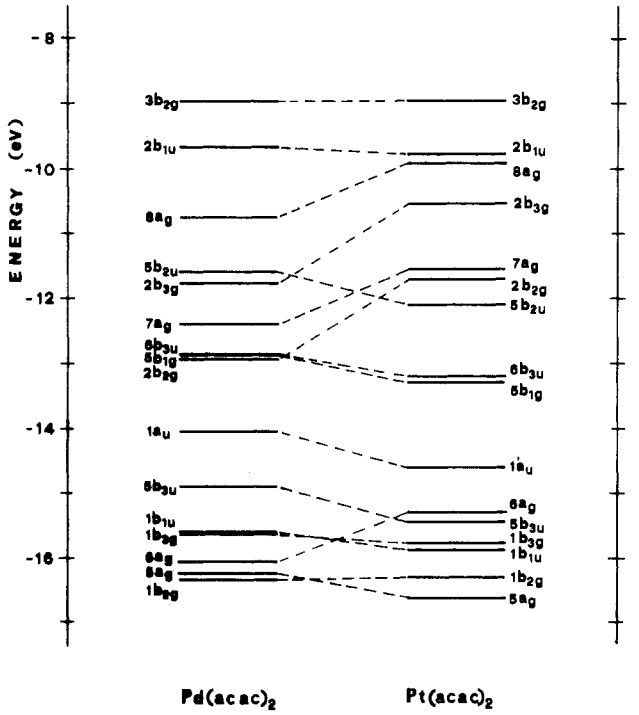

Figure 6. Correlation diagram between ground-state valence eigenvalues of $Pd(acac)_2$ and $Pt(acac)_2$.

MO's are observed (Tables I and IV and Figure 6).

Moreover, inspection of the correlation diagram in Figure 6 indicates that almost all the MO's that posses metal–ligand bonding ($5a_g$, $1b_{3g}$, $5b_{1g}$) and nonbonding ($1b_{1u}$, $5b_{3u}$, $1a_u$, $6b_{3u}$, $5b_{2u}$, $2b_{1u}$) character are more stable while those having an antibonding ($2b_{2g}$, $7a_g$, $2b_{3g}$, $8a_g$) metal–ligand nature are less stable than those in $Pd(acac)_2$.

An adequate rationale to these observations can be found both in the stronger metal–ligand σ and π interactions, as indicated by the Pt–O overlap population in Table IV, and in stronger ligand-to-metal charge transfer to metal 6s virtual atomic orbital (Table II), which reduces the negative charge over the ligand framework.

The PE spectra of $Pt(acac)_2$ (Figures 7, 8) present remarkable analogies with those of $Pd(acac)_2$, thus consisting of 10 bands in the region up to 12 eV.

As in the case of $Pd(acac)_2$, a satisfactory agreement is found between experimental IE's and PSHONDO eigenvalues corrected for reorganization effects (both ΔSCF and PT) in the various ion states (Table V).

However, we note that, given the greater He II cross section for Pd 5d-based MO's, He I vs. He II intensity data (vide infra) suggest an inverted sequence (and hence an inverted assignment) in the case of $8a_g$ and $3b_{2g}$ MO's. In fact, band B, which increases remarkably in the He II spectrum (Table V), certainly represents

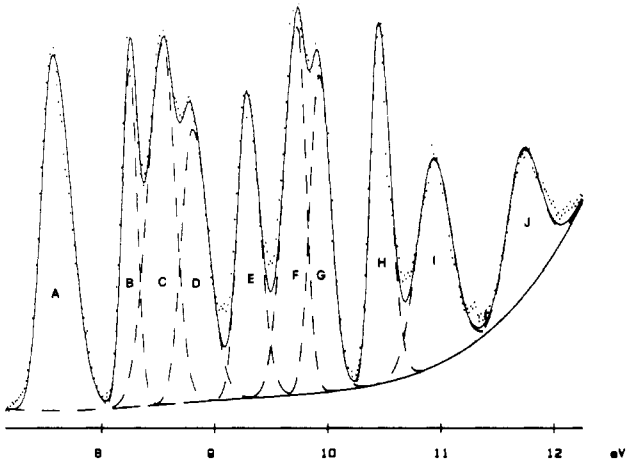

Figure 7. He I spectrum of $Pt(acac)_2$ in the low-IE region: experimental spectrum (point lines), Gaussian components (dashed lines), convolution of Gaussian components (solid line).

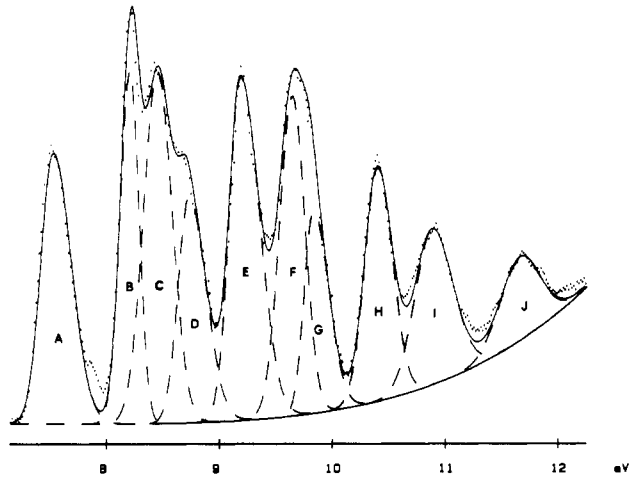

Figure 8. He II spectrum of $Pt(acac)_2$ in the low-IE region: experimental spectrum (point lines), Gaussian components (dashed lines), convolution of Gaussian components (solid line).

the ionization from the $8a_g$ MO, in accordance with its high metal 5d character (Table IV), while band A, whose intensity does not change, must be related to the $3b_{2g}$ MO's (Table V). For the bands that follow up to 12 eV (C–J) we propose the assignments listed in Table V. The He I vs. He II intensity changes of these bands (Table V) are perfectly tuned with the composition of the corresponding MO's (Table IV).

Figure 9 pictures a correlation diagram between experimental IE's of corresponding bands in the spectra of $Pd(acac)_2$ and $Pt(acac)_2$.

A trend of experimental IE's analogous to that observed with ground-state eigenvalues (Figure 6) is found. In particular, higher

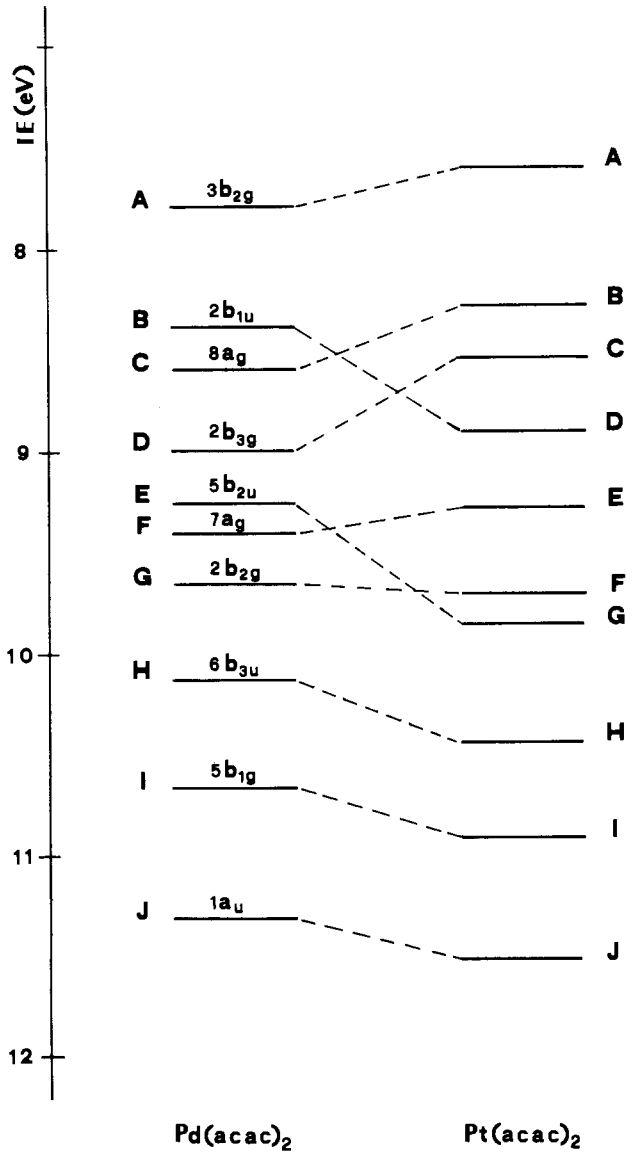

Figure 9. Correlation diagram between experimental IE's of $Pd(acac)_2$ and $Pt(acac)_2$.

IE's are associated to all the MO's possessing nonbonding or metal–ligand bonding character while lower values are associated with those MO's having antibonding metal–ligand nature.

Concluding Remarks

This paper presents a study of the electronic structure of square-planar complexes using theoretical ab initio calculations and combined He I and He II PE spectroscopy.

The pseudopotential ab initio method, in connection with a first-order perturbative approach to correct the Koopmans' eigenvalues for the reorganization effects upon ionization, has proven capable of providing a suitable rationale to the PE data with relatively low computational efforts. The relative intensity changes of various PE bands on passing from the He I to the He II excited PE spectra have proven, however, to be of crucial guidance for the final assignments.

Sizable interactions involving almost all the upper filled MO's of the ligand cluster and the metal d orbitals of suitable symmetry emerge from the analysis of the ab initio results of $Pd(acac)_2$. Those due to ligand orbitals of π symmetry mainly involve filled metal $4d_{xz}$ and $4d_{yz}$ orbitals and, although of relevance, do no result in significant metal–ligand overlap population because contributions due to filled bonding and antibonding counterparts tend to cancel each other. The interactions due to orbitals of σ symmetry involve empty $4d_{xy}$ and 5s metal orbitals and result in a positive metal–ligand overlap population. There is no evidence of any significant metal-to-ligand back-donation, and therefore, the acac anion can be considered as a predominantly σ-donor ligand.

As expected,[2a,b,9j] a larger metal–ligand covalency has been found in the case of $Pt(acac)_2$ and the greater ligand-to-metal σ donation results in a less positive charge (than in $Pd(acac)_2$) associated to the Pt atom.

The energy sequence of the states produced upon ionization are largely dominated by reorganization effects in the ion. Of course, repolarization energies parallel the metal d-orbital contribution to a particular MO and are large enough to upset the energy sequence of ground-state MO's. Moreover, significant repolarization energies have been found associated also with MO's having a dominant O_{2p} lone-pair character. This observation suggests that in the assignment of PE spectra of those complexes whose upper filled MO's crowd the valence region, the evaluation of reorganization energies must include those associated with ligand-based MO's having lone-pair character.

Finally, within a purely PE spectroscopy context, we must mention that the present data support the earlier contention that, at the He II wavelength, the cross section of MO's having a metal 4d contribution is greater than in the case of those having 5d character.[35]

Further investigations are in progress[36] on various other classes of square-planar complexes to clarify the relationships between the chemical structure and the bonding capabilities of the various ligands.

Acknowledgment. We gratefully acknowledge Dr. J. P. Daudey (Université P. Sabatier, Toulouse, France) for providing the PSHONDO code. The financial support of the Consiglio Nazionale delle Ricerche (CNR, Rome, Italy) and of the Ministero della Pubblica Istruzione (MPI, Rome, Italy) is also gratefully acknowledged.

Registry No. $Pd(acac)_2$, 14024-61-4; $Pt(acac)_2$, 15170-57-7.

Supplementary Material Available: A listing of the Gaussian basis sets (2 pages). Ordering information is given on any current masthead page.

(35) See for example: Egdell, R. G.; Orchard, A. F. *J. Chem. Soc., Faraday Trans. 2* **1978**, *74*, 485. Egdell, R. G.; Orchard, A. F. *J. Electron Spectrosc. Relat Phenom.* **1978**, *14*, 277.

(36) Di Bella, S.; Fragalà, I.; Granozzi, G., work in progress.